

Global Simulation of Linear Instability in W7-X and LHD with EUTERPE

J. Riemann¹, R. Kleiber¹, M. Borchardt¹

¹ *Max-Planck-Institut für Plasmaphysik, D-17491 Greifswald, Germany*

EUTERPE is a global (full radius, full flux surface) gyro-kinetic particle-in-cell (PIC) code which is applied to the numerical simulation of plasmas in three-dimensional (3D) magnetic field configurations. The code is capable of simulating up to three kinetic species (ions, electrons and fast particles/impurities) and solves the field equations for the electrostatic and parallel vector potentials. EUTERPE can be operated in different modes - e.g. electrostatic or fully electromagnetic - and can also neglect or take into account the non-linearity [1]. As the code is applied by several users, different efforts have been made to implement a growing complexity of physics. Recent developments included collisions [2] and impurity transport [3]. To study energy transfer between fast particles and MHD modes, EUTERPE was also coupled to the reduced MHD code CKA [4], and an electron-fluid model was developed [5]. In this manner, EUTERPE has become a valuable tool for the analysis of a wide range of plasma instabilities (ITG, ETG, TEM, GAE, TAE ...) which in particular can help to identify non-local effects. With respect to the upcoming operation phase of the Wendelstein 7-X stellarator, there is a growing interest to establish EUTERPE as a reliable modelling tool which can be used to assist the numerical reconstruction and interpretation of experimental findings.

This contribution gives a preliminary overview of results obtained from the simulation of linear ion-temperature-gradient (ITG) driven instabilities in stellarators, in particular Wendelstein 7-X (W7-X) and the Large Helical Device (LHD). The aim of these studies was to obtain basic information on expected modes, e.g. growth rates, mode numbers, mode structure, frequencies etc., from systematic scans over both temperature and density gradients. As a starting point for such investigations, the following simplifications and assumptions were made: (i) As mentioned above, only the linear regime was considered, thus neglecting all contributions to the equations of motion for the gyrating particles that in general depend on the fluctuating electrostatic potential ϕ . (ii) Using adiabatic electrons resulted in further simplification and allowed for a larger time step to speed up the computations. (iii) Finally, certain assumptions were made w.r.t. the temperature and density profiles used. EUTERPE runs are routinely performed using 3D equilibrium results from the VMEC code. As VMEC results are based on prescribed equilibrium pressure profiles, self-consistent EUTERPE runs should use the same pressure profiles. However, it is common practice so far to vary densities and temperatures independently, thus

assuming that the magnetic configuration would not change under these modifications. The results presented here were obtained following two different approaches. In a first step (“phase I”), a prescribed equilibrium configuration was assumed not to be sensitive to the modifications applied to temperature and density profiles while scanning through their gradients over a certain range of scale lengths L_T and L_n . Profiles were described by piece-wise linear (triangular) functions $d\ln T/ds$ and $d\ln n/ds$, where s is the normalized toroidal flux. Results obtained in this way are rigorously speaking not consistent with the underlying equilibrium configuration, but provide a first picture of linear ITG behaviour. Figure 1 compares the stability diagrams obtained for W7-X ($\beta = 2\%$) and LHD ($\beta = 1.5\%$). In both cases the reference temperature at the radial position $s_* = 0.5$ was $T_* = 1\text{keV}$.

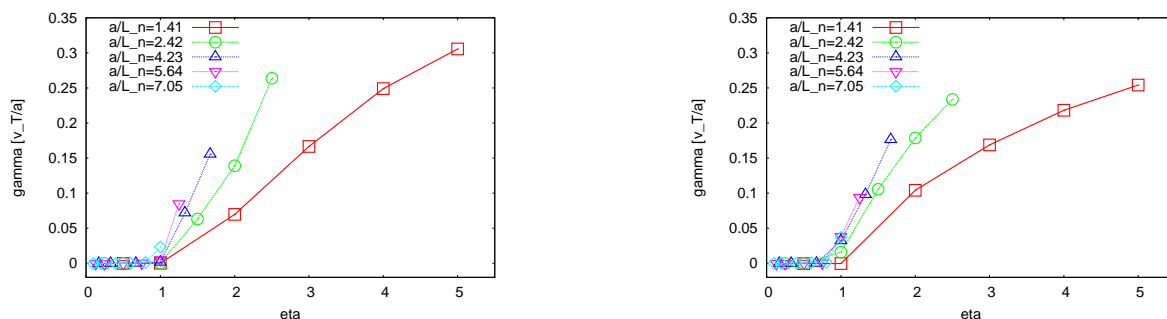


Figure 1: “Phase I” stability diagrams for W7-X (left) and LHD (right). The plots show the normalized growth rates $\gamma/(v_T/a)$ for linear ITG instability as a function of the stability parameter $\eta_i = (L_n/L_T)_i$, with thermal velocity v_T and minor radius $a = 0.5\text{m}$ (W7-X) and 0.6m (LHD).

The most obvious result is the existence of a clear threshold for linear ITG instability at $\eta_i \approx 1$. Furthermore, the absolute growth rates for the two devices are found to be similar. Besides their growth rates, it is also of interest where the fluctuations appear and how far they extend.

Figure 2 shows a typical pattern for an ITG mode in W7-X obtained with “phase I” profiles.

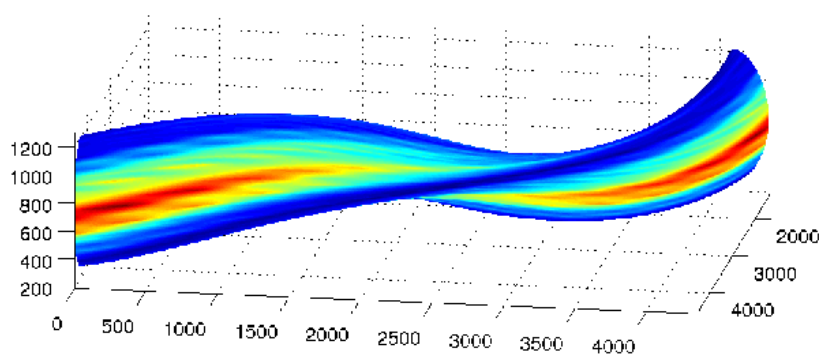


Figure 2: Normalized electrostatic potential on a flux surface $s = 0.5$ for ITG in W7-X.

The potential fluctuations are seen to reside on the outside of the torus, in the region of unfavourable curvature, where they avoid the helical high-shear edge limiting the toroidal extension of the mode.

In the interest of more realistic modelling, the profiles used for the EUTERPE runs were modified in “phase II” in order to meet the requirement for consistency with an underlying equilibrium. In a fully realistic calculation, an equilibrium would be derived from experimental data or transport simulations. The following results were obtained with “quasi-realistic” profiles being consistent with the equilibrium (the ones already used in “phase I”) but remain simplified w.r.t. the actual shape of the profiles. We assume $p = p_e + p_i = 2nT$ and write

$$\frac{n}{n_0} = \left(\frac{p}{2p_0} \right)^\chi \quad \text{and} \quad \frac{T}{T_0} = \left(\frac{p}{2p_0} \right)^{1-\chi} \quad \longrightarrow \quad \eta = \frac{d \ln T}{ds} / \frac{d \ln n}{ds} = \frac{1-\chi}{\chi} \quad , \quad (1)$$

where $p = p(s)$ is the pressure profile used for the equilibrium configuration. There is then no need to recalculate the magnetic field, and η_i is a constant over the radius determined by the free parameter χ . The “phase II” results thus describe a “configuration characteristic”, i.e. a scan over different combinations of temperature and density being consistent with one prescribed equilibrium pressure profile.

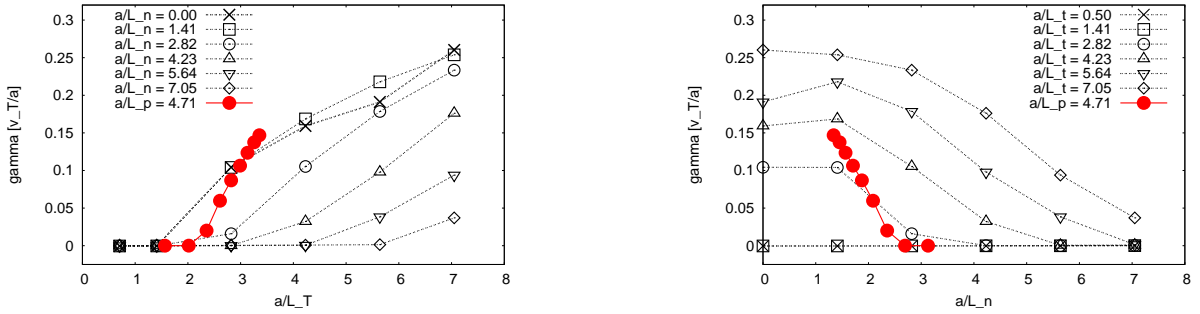


Figure 3: Linear growth rates $\gamma/(v_T/a)$ vs. a/L_T (left) and a/L_n (right) in LHD for the scan along a configuration characteristic (red dots) as compared to “phase I” (black) results. ($a = 0.6\text{m}$)

Figure 3 shows the linear ITG growth rates for different combinations of a/L_T and a/L_n for a given pressure profile ($p/p_0 = 1 - 2s + s^2$) in LHD with $\beta = 1.5\%$, covering a range of $0.5 \leq \eta_i \leq 2.5$. The profiles used in these simulations are not yet fully consistent with the underlying equilibrium. The reason is that we had to introduce finite residual temperatures and densities at $s = 1$ to avoid infinite values for T'/T and n'/n . Here, we used a residual pressure $\delta p = 0.05p_0$, whereas the equilibrium was calculated assuming $p|_{s=1} = 0$. The growth rates are found to be sensitive to the actual value δp , and for realistic modelling one needs to involve physically reasonable equilibrium pressures at the boundary $s = 1$.

Figure 4 compares two cuts through the LHD plasma at constant toroidal angle $\varphi = 0$. The left

plot shows the structure of an ITG mode for $\eta_i = 2.0$ with $m_0/n_0 = 120/81$ residing around $s \approx 0.61$. The right one corresponds to $\eta_i = 1.0$ with $m_0/n_0 = 160/92$ at $s \approx 0.75$. The growth rates are $\gamma|_{\eta_i=2.0} = 0.124v_T/a$ and $\gamma|_{\eta_i=1.0} = 0.021v_T/a$. As in fig. 2, the modes reside at the outer mid-plane around $\theta = 0$. For $\eta_i = 2.0$, the mode is clearly shifted below the equatorial plane – a characteristic feature observed in all global simulations so far. For $\eta_i = 1.0$, the mode is shifted outwards and the scale of the fluctuations is smaller. Note that the potentials (absolute values) are normalized to their maximum, and the mode is actually almost stable.

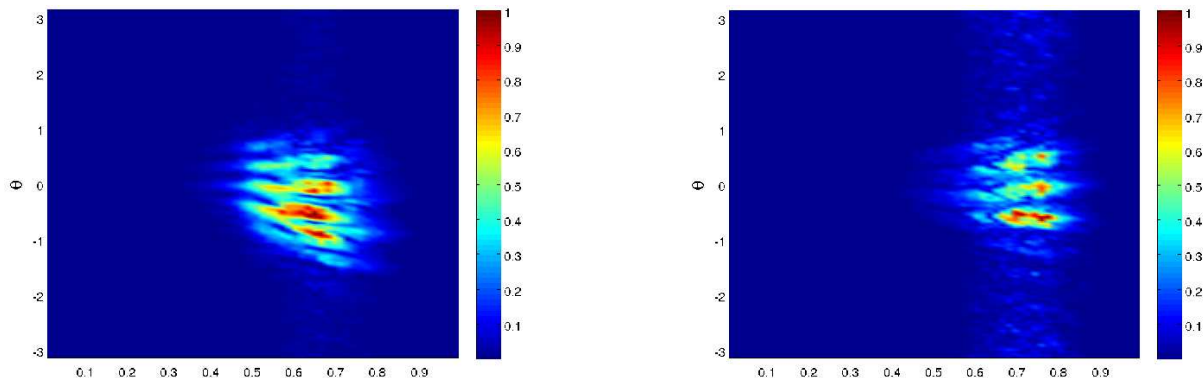


Figure 4: Normalized electrostatic potential at $\varphi = 0$ in LHD for $\eta_i = 2.0$ (left) and $\eta_i = 1.0$ (right).

Figure 5 shows the corresponding mode patterns on a flux surface in LHD. Again, the mode on the right is almost stable. Similar studies for Wendelstein 7-X are underway.

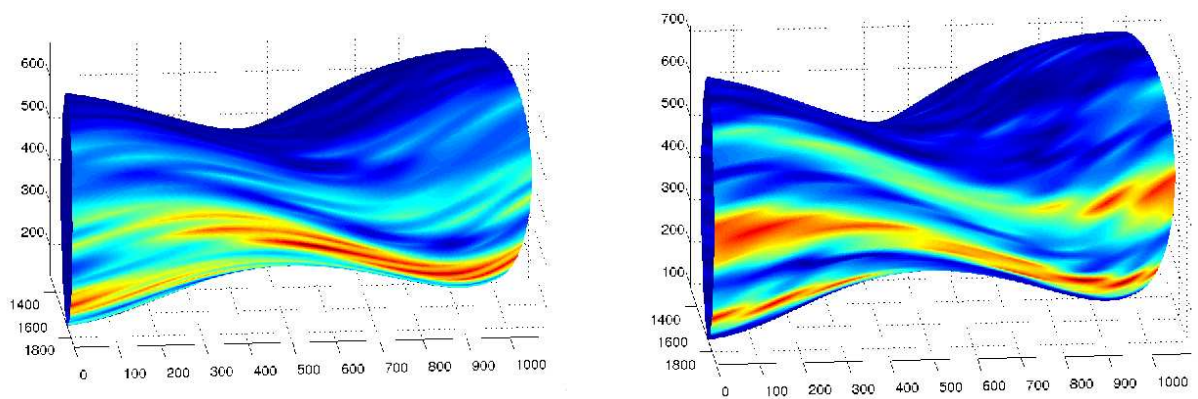


Figure 5: Normalized electrostatic potential at $s = 0.61$ (0.75) for $\eta_i = 2.0$ (left) and $\eta_i = 1.0$ (right).

References

- [1] V. Kornilov, R. Kleiber, R. Hatzky, L. Villard and G. Jost, PoP **11**, 3196 (2004)
- [2] K. Kauffmann, R. Kleiber, R. Hatzky, M. Borchardt, Journ. Phys. **260**, 012014, (2010)
- [3] J. M. García-Regaña et al., Plas. Phys. Contr. Fusion **55** 074008 (2013)
- [4] T. Feher, Thesis, IPP Report 13/22 (2014)
- [5] M. Cole et al., *submitted to PoP* (2014)